Applications of Mathematics

Nishi Deepa Palo; Jasobanta Jena; Meera Chadha

Development of small and large compressive pulses in two-phase flow

Applications of Mathematics, Vol. 69 (2024), No. 2, 233–255

Persistent URL: http://dml.cz/dmlcz/152314

Terms of use:

© Institute of Mathematics AS CR, 2024

Institute of Mathematics of the Czech Academy of Sciences provides access to digitized documents strictly for personal use. Each copy of any part of this document must contain these *Terms of use*.

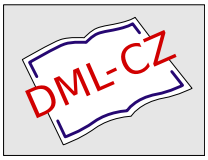

This document has been digitized, optimized for electronic delivery and stamped with digital signature within the project *DML-CZ: The Czech Digital Mathematics Library* http://dml.cz

69 (2024) APPLICATIONS OF MATHEMATICS No. 2, 233–255

DEVELOPMENT OF SMALL AND LARGE COMPRESSIVE PULSES IN TWO-PHASE FLOW

Nishi Deepa Palo, New Delhi, Jasobanta Jena, Bhubaneswar,
Meera Chadha, New Delhi

Received May 23, 2023. Published online January 23, 2024.

Abstract. The evolutions of small and large compressive pulses are studied in a two-phase flow of gas and dust particles with a variable azimuthal velocity. The method of relatively undistorted waves is used to study the mechanical pulses of different types in a rotational, axisymmetric dusty gas. The results obtained are compared with that of nonrotating medium. Asymptotic expansion procedure is used to discuss the nonlinear theory of geometrical acoustics. The influence of the solid particles and the rotational effect of the medium on the distortion are investigated. In a rotational flow it is observed that with the increase in the value of rotational parameter, the steepening of the pulses also increases. The presence of dust in the rotational flow delays the onset of shock formation thereby increasing the distance where the shock is formed first. The rotational and the dust parameters are observed to have the same effect on the shock strength.

Keywords: hyperbolic system of equations; shock waves, asymptotic expansion

MSC 2020: 35A18, 35B40

1. Introduction

Rotational flow occurs in nature as well as in many industrial processes like power plants, chemical plants, oil and gas industries, etc. These mainly involve multi-phase flow. A detailed understanding of the flow characteristics is required for the design and optimization of industrial devices and processes as well as for safety considerations of multi-phase flow systems. Computational fluid dynamics (CFD) can be used to provide such detailed information.

The two-phase flow of a mixture of solid particles and a fluid in which the solid particles occupy less than 5% of the total volume of the mixture and mix well with the fluid in the flow field is called a pseudo-fluid [9]. The mixture of solid particles

DOI: 10.21136/AM.2024.0107-23

© Institute of Mathematics, Czech Academy of Sciences 2024.

and gases are of great interest due to its broad applications in many areas like geophysics, astrophysics, plasma physics, nuclear power plant and blast waves [19]. Study of lunar ash flow, volcanic and cosmic explosions, description of star formation and nuclear explosions are its recent applications.

The theory of relatively undistorted waves was first developed by Varley and Cumberbatch [14], where they used the method to discuss finite amplitude, radially symmetric, isentropic waves in fluids. Parker and Seymour [11] used this theory to study finite amplitude pulses in an inhomogeneous granular material. Radha and Sharma [12] studied wave propagation and interaction in a relaxing gas using this method. Jena and Sharma [5] discussed the different modes of wave propagation in a nonideal gas using this theory. Chadha and Jena [2] have taken nonideal medium in presence of dust particles to study the behaviour of mechanical pulses. In all of the above mentioned literatures, the nonrotational flow of the medium was considered. In this paper, we study the evolution of weak pulses in a mixture of small solid particles and gas (pseudo-fluid) in a cylindrically symmetric rotational flow. The theory of relatively undistorted wave and the asymptotic expansion methods are used to study the mechanical pulses of different types. The rotational effects for weak pulses are analysed for a pseudo-fluid rotating with constant angular velocity and variable azimuthal velocity.

A flow in which the fluid particles rotate about their own axes while flowing is called a rotational flow. In recent decades the study of nonideal rotational flow has become important due to its widespread applications ranging from the study of the wind flow above the atmospheric boundary layer with negligible shear force to the study of explosions in rotating stars. Chaturani [4] considered the rotational flow to study the propagation of spherical shock waves. Levin et al. [6] studied the detonation wave propagation in rotational gas flows. Vishwakarma and Nath [17] obtained the self-similar solutions for cylindrical shock waves in the presence of heat conduction and radiation heat flux for a rotational dusty gas. Nath et al. [8] studied the self similar solution for the flow behind an exponential shock wave in a rotational axisymmetric flow with magnetic effect. Sahu [13] discussed the propagation of an exponential shock wave in a rotational axisymmetric isothermal and adiabatic flow of a self-gravitating, nonideal gas under the influence of axial and azimuthal magnetic field. He extended the idea of introducing self-gravitation in the model.

In this paper, we study the evolution of weak pulses in a mixture of small solid particles and gas (pseudo-fluid) in a cylindrically symmetric rotational flow. The theory of relatively undistorted wave and the asymptotic expansion methods are used to study the mechanical pulses of different types. The rotational effects for weak pulses are analysed for a pseudo-fluid rotating with constant angular velocity and variable azimuthal velocity.

2. Governing equations

The governing equations describing one-dimensional, adiabatic, unsteady flow of a mixture of a gas and small solid particles are based on assumptions made in [2], [16], [1]. Some of these assumptions are: (i) the solid particles present in the fluid are spherical in shape, (ii) they are small in size and identical so that the presence of these particles does not affect the kinetic property of the gas and (iii) the medium has variable azimuthal velocity. The system of partial differential equations describing the cylindrically symmetric rotation about the axis of symmetry with small dust particles is given by

$$
\begin{aligned}
&\varrho_t + u\varrho_r + \varrho u_r + \frac{\varrho u}{r} = 0,\\
&u_t + uu_r + \frac{p_r}{\varrho} - \frac{v^2}{r} = 0,\\
&p_t + up_r + a^2\varrho\Big(u_r + \frac{u}{r}\Big) = 0,\\
&v_t + uv_r + \frac{uv}{r} = 0,
\end{aligned}
\tag{2.1}
$$

where r is the radial distance, t is the time, ϱ is the density of the mixture, u is the radial component of the velocity, p is the pressure, v is the azimuthal component of the velocity and is given by $v = \Omega r$ with Ω as the angular velocity of the medium. The equilibrium speed of sound is given by $a^2 = \Gamma p/(\varrho(1-Z))$ [10], where $Z = V_{sp}/V_g$ is the volume fraction of solids with V_{sp} and V_g being the volume of solid particles and the total volume of the mixture [3], respectively. The Grüneisen coefficient is given by $\Gamma = (\gamma(1+\chi\beta))/(1+\chi\beta\gamma)$, γ is the adiabatic index, $\chi = k_p/(1-k_p)$. The mass fraction of the solid particles present in the mixture is k_p, given by $k_p = m_{sp}/m_T$, m_{sp} being the mass of the solid particles and m_T being the total mass of the mixture. Here, $\beta = c_{sp}/c_p$, where c_{sp} is the specific heat of solid particles and c_p is the specific heat of gas at constant pressure. The ratio of the density of the solid particles to the species density of the gas is given by $G = \varrho_{sp}/\varrho_g$. The two parameters k_p and G are related by the relation $Z = \theta\varrho$, $\theta = k_p/\varrho_{sp}$, ϱ_{sp} is the density of the solid particles. The equation of state is given by

$$
p = \frac{1-k_p}{1-Z}\varrho R\mathcal{T},
\tag{2.2}
$$

where R denotes the gas constant and $\mathcal{T}$ is the temperature of the mixture. When the mass fraction $k_p = 0$, it refers to the dust free medium. Also, when $Z = 0$, then $\Gamma = \gamma$ and $a^2 = \gamma p/\varrho$ and the mixture becomes an ideal gas. Ideal gas means that the dust particles interaction in the medium is not taken into account.

We express the system of equations (2.1) in the matrix form as

$$\partial_t U_i + A_{ij}\partial_r U_j + B_i = 0, \quad i,j = 1,2,3,4. \tag{2.3}$$

Here, U_i and B_i are the components of column vectors U and B defined as $U = (\varrho, u, p, v)^\top$, $B = (\varrho u/r, v^2/r, a^2\varrho u/r, vu/r)^\top$, $\top$ denotes transposition, and A_{ij} are the components of 4×4 matrix A defined as $A_{11} = A_{22} = A_{33} = A_{44} = u$, $A_{12} = \varrho$, $A_{23} = 1/\varrho$, $A_{32} = p\Gamma/(1-\theta\varrho)$, $A_{13} = A_{14} = A_{21} = A_{24} = A_{31} = A_{34} = A_{41} = A_{42} = A_{43} = 0$.

3. Theory of relatively undistorted wave

A wave is said to be relatively undistorted in $U(r,t)$ with respect to r if there exists a family of propagating wavelets $\zeta(r,t) =$ constant such that the magnitudes of the rate of change of vector $U(r,t)$ with r moving with the wavelets is negligible in comparison to the magnitude of the rate of change of U at fixed t. If $t = \tau(r,\zeta)$ denotes the time of arrival of the wavelets ζ at r and if $\varphi(r,\zeta) = U(r,\tau(r,\zeta))$, then in a relatively undistorted wave [15]

$$\Big\|\frac{\partial\varphi_i}{\partial r}\Big\| \ll \Big\|\frac{\partial U_i}{\partial r}\Big\|. \tag{3.1}$$

Since $\partial\varphi/\partial r = \partial U/\partial r + (\partial\tau/\partial r)\partial U/\partial t$, in a relatively undistorted wave $\partial U/\partial r \simeq -(\partial\tau/\partial r)\partial U/\partial t$ [14] and hence,

$$\Big|\frac{\partial\varphi_i}{\partial r}\Big| \ll \Big|\frac{\partial U_i}{\partial t}\Big|.$$

Using the transformation from (r,t) to (r,ζ), the system of equations (2.3) can be written in the form

$$\Big(A_{ij}\frac{\partial\tau}{\partial r} - \delta_{ij}\Big)\frac{\partial U_j}{\partial\tau} = A_{ij}\frac{\partial\varphi_j}{\partial r} + B_i, \tag{3.2}$$

where δ_{ij} is the Kronecker function. The above equations are compatible if

$$\|B\| = \mathcal{O}\Big(\Big\|A_{ij}\frac{\partial\varphi_j}{\partial r}\Big\|\Big) \tag{3.3}$$

where $(\partial\tau/\partial r)^{-1}$ is the characteristic values of the matrix A. When the determinant $\|A_{ij} - \delta_{ij}(\partial\tau/\partial r)^{-1}\| = 0$, φ_i must satisfy the compatibility condition

$$L_i\Big(A_{ij}\frac{\partial\varphi_j}{\partial r} + B_i\Big) = 0 \tag{3.4}$$

for every left eigenvector L_i of A associated with the eigenvalue $t(\partial\tau/\partial r)^{-1}$. Taking the first approximation of equations (3.2) subject to the compatibility conditions we get

$$\Big(A_{ij} - \delta_{ij}\Big(\frac{\partial\tau}{\partial r}\Big)^{-1}\Big)\frac{\partial\varphi_j}{\partial\zeta} = 0. \tag{3.5}$$

Equation (3.5) can be expressed as

$$\frac{\partial\varphi_i}{\partial\zeta} = \vartheta(\zeta, r)\mathcal{R}_i, \tag{3.6}$$

where $\mathcal{R} = (\mathcal{R}_i)$ represents the right eigenvector of A associated with the eigenvalue $(\partial\tau/\partial r)^{-1}$ and ϑ is a scalar.

The matrix A in (2.3) has eigenvalues $u \pm a$ and u (of multiplicity two). We consider the solution in the region $r > 0$, where the motion consists of only one component of the wave. The wave associated with the largest eigenvalue is perturbed at the boundary $r = r_0$ by an applied pressure $p(r_0, t) = \psi(t)$. The left and right eigenvectors associated with the largest eigenvalue $(\partial\tau/\partial r)^{-1} = u + a$ are given by

$$L = (0, a\varrho, 1, 0) \quad \text{and} \quad \mathcal{R} = (\varrho, a, a^2\varrho, 0)^\top. \tag{3.7}$$

3.1. Disturbances of finite amplitude. Consider a region ahead of which the disturbance $\zeta(r, t) = 0$ is propagating in a uniform state of rest. The flow variables in the undisturbed state are

$$u = u_0 \equiv 0, \quad p = p_0(r), \quad \varrho = \varrho_0, \quad v = v_0(r). \tag{3.8}$$

For fixed r, the angular velocity Ω_0 is constant meaning there is no acceleration. Taking $v_0 = \Omega_0 r^\lambda$ (see [17]), $0 < \lambda < 1$ and using (3.8), we obtain the following form of p_0 from $(2.1)_2$:

$$p_0 = \alpha r^{2\lambda}, \quad \text{where} \quad \alpha = \frac{\varrho_0\Omega_0^2}{2\lambda}. \tag{3.9}$$

Without loss of generality, ζ of each wavelet is taken so that $\zeta = t$ on $r = r_0$. Hence, at $t = t_0$, the boundary conditions for p and τ are given by

$$p = \psi(\zeta), \quad \tau = \zeta. \tag{3.10}$$

The relation (3.6) (determine the conditions in the wave region associated with the eigenvalue $u+a$) are integrated subject to the conditions (3.8) leading to the following

forms of ϱ, u, a and v:

$$\varrho = \varrho_0\Big(\frac{p}{p_0}\Big)^{1/\Gamma}\Big\{1 - Z_0\Big(1 - \Big(\frac{p}{p_0}\Big)^{1/\Gamma}\Big)\Big\}^{-1}, \tag{3.11}$$

$$u = \frac{2a_0(1-Z_0)}{(\Gamma-1)}\Big(-1 + \Big(\frac{p}{p_0}\Big)^{(\Gamma-1)/(2\Gamma)}\Big),$$

$$a = a_0\Big(\frac{p}{p_0}\Big)^{(\Gamma-1)/(2\Gamma)}\Big(1 - Z_0 + Z_0\Big(\frac{p}{p_0}\Big)^{1/\Gamma}\Big), \quad v = v_0.$$

Using (3.2), (3.7), (3.11) and the relation $(\partial\tau/\partial r)^{-1} = u + a$, we obtain the following transport equations for p and τ:

$$\frac{\partial p}{\partial r} - \frac{\lambda p}{r} + \frac{\Gamma r^{2\lambda-1}\alpha}{2(\Gamma-1)}\Big(\frac{p}{p_0} - \Big(\frac{p}{p_0}\Big)^{(\Gamma+1)/(2\Gamma)}\Big) + \frac{1}{2rh(p)}\Big(\frac{p}{p_0}\Big)^{(\Gamma+1)/(2\Gamma)} \tag{3.12}$$

$$\times\Big\{\frac{a_0^2\varrho_0(1-Z_0)}{\Gamma-1}\Big(\Big(\frac{p}{p_0}\Big)^{(\Gamma-1)/\Gamma}\Big(1 - Z_0 + Z_0\Big(\frac{p}{p_0}\Big)^{1/\Gamma}\Big)$$

$$-\Big(\frac{p}{p_0}\Big)^{(\Gamma-1)/(2\Gamma)}\Big) - \varrho_0 v_0^2\Big\} = 0,$$

$$\frac{\partial\tau}{\partial r} = \frac{1}{a_0 h(p)},$$

where

$$h(p) = \frac{2(1-Z_0)}{\Gamma-1}\Big(-1 + \Big(\frac{p}{p_0}\Big)^{(\Gamma-1)/(2\Gamma)}\Big) + \Big(\frac{p}{p_0}\Big)^{(\Gamma-1)/(2\Gamma)}\Big(1 - Z_0 + Z_0\Big(\frac{p}{p_0}\Big)^{1/\Gamma}\Big).$$

Equation $(3.12)_1$ can be integrated along with the boundary condition given by equation $(3.10)_1$ to yield p. Using p in equation $(3.12)_2$ and then integrating, τ can be obtained. The other flow variables ϱ, u and a can be evaluated from (3.11) using the obtained value of p and p_0 from (3.9). Integration of equation $(3.12)_2$ leads to evaluation of the location of ζ wavelets in the form

$$\tau = \zeta + \int_{r_0}^{r} \kappa(x, \psi(\zeta))\,\mathrm{d}x, \tag{3.13}$$

where $\kappa = \{a_0 g(p(r, \psi(\zeta)))\}^{-1}$ with g being a function of $p(r, \psi(\zeta))$. The relation (3.13) implies that there exists a point r_s, where a shock forms on the wavelet ζ_s and is given by the relation

$$1 + \frac{\mathrm{d}\psi}{\mathrm{d}\zeta}\int_{r_0}^{r_s} \frac{\partial\kappa}{\partial\psi}(s, \psi(\varphi_s))\,\mathrm{d}s = 0. \tag{3.14}$$

It may be noted that the above results are significant as both the amplitude and the shock formation along any wavelet depend on the amplitude $\psi(\zeta)$ carried out by that wavelet. The implications of the same are discussed in the following subsections.

3.2. The waves with small amplitude. For weak disturbances the nonlinear equations are often linearized by neglecting all but the first order powers of the perturbations [19]. These disturbances, however small they may be, become crucial after sufficient time. Considering the small perturbations in the flow variables, we linearize equations (3.12) about the uniform state (3.10) as per the requirement of small amplitude limit and obtain

$$\frac{\partial p^{(1)}}{\partial r} + \frac{(1-\lambda)p^{(1)}}{2r} = 0, \quad \frac{\partial \tau}{\partial r} = \frac{1}{a_0}\Big(1 - \frac{\Gamma+1}{2\Gamma}\frac{p^{(1)}}{p_0}\Big), \tag{3.15}$$

where $p^{(1)}$ is the small perturbation to p_0. From the boundary conditions (3.10), we obtain the following boundary conditions for $p^{(1)}$ at $r = r_0$:

$$p^{(1)} = \widetilde{\psi}(\zeta), \quad \tau = \zeta, \tag{3.16}$$

where $|\widetilde{\psi}(\zeta)| = |\psi(\zeta) - p_0| \ll 1$. Integration of equations (3.15) with respect to the boundary conditions (3.16) leads to

$$p^{(1)} = \widetilde{\psi}(\zeta)\Big(\frac{r}{r_0}\Big)^{-(1-\lambda)/2}, \tag{3.17}$$

$$K_1(\tau-\zeta) = r_0^{1-\lambda}\Big\{\frac{1}{(1-\lambda)}\Big(\Big(\frac{r}{r_0}\Big)^{1-\lambda} - 1\Big)\Big\} - r_0^{1-3\lambda}\Big\{\widetilde{\psi}(\zeta)K_2\Big(\Big(\frac{r}{r_0}\Big)^{(1-5\lambda)/2} - 1\Big)\Big\},$$

where

$$K_1 = \Big(\frac{\Gamma}{2\lambda(1-Z_0)}\Big)^{1/2}\Omega_0, \quad K_2 = \frac{2(\Gamma+1)}{\Gamma\alpha(1-5\lambda)}.$$

Equation $(3.17)_2$ confirms that a shock will first form at (r_s, ζ) and the minimum value of the location r_s can be obtained from the solution of

$$S(x) = 1 - K_2K_1^{-1}\frac{\mathrm{d}\widetilde{\psi}}{\mathrm{d}\zeta}r_0^{1-3\lambda}\Big(\Big(\frac{r}{r_0}\Big)^{(1-5\lambda)/2} - 1\Big) = 0. \tag{3.18}$$

The shock once evolved will propagate separating the continuous region. The equal area rule [18] is used to find the location of the weak shock. From the equal area rule we get

$$2\int_{\zeta_1}^{\zeta 2} \widetilde{\psi}(t)\,\mathrm{d}t = (\zeta_2 - \zeta_1)(\widetilde{\psi}(\zeta_1) + \widetilde{\psi}(\zeta_2)), \tag{3.19}$$

where ζ_1 and ζ_2 are the wavelets ahead and behind the shock. For a weak shock the impact of the advance wavelet is negligible, hence, $\zeta_1 = 0$ and $\widetilde{\psi}(\zeta_1) = 0$.

Equation (3.19) in view of equation $(3.17)_2$ can be written as

$$\int_0^{\zeta_2} \widetilde{\psi}(t)\,\mathrm{d}t = \frac{2(\Gamma+1)\widetilde{\psi}^2(\zeta_2)r_0^{1-3\lambda}}{K_1\Gamma(1-5\lambda)\alpha}\Big(\Big(\frac{r}{r_0}\Big)^{(1-5\lambda)/2} - 1\Big). \tag{3.20}$$

From equation (3.20) we observe that when r increases, $\widetilde{\psi}(\zeta_2)$ varies as $\Upsilon^{-1/2}$, where

$$\Upsilon = r_0^{1-3\lambda}\Big(\Big(\frac{r}{r_0}\Big)^{(1-5\lambda)/2} - 1\Big). \tag{3.21}$$

More precisely,

$$[p] \sim \widetilde{r}^{-3(1-7\lambda)/4}, \quad \text{where } \widetilde{r} = \frac{r}{r_0}. \tag{3.22}$$

The result in equation (3.22) is in conformity with the result obtained by Whitham ([18], page no. 9, equation (19)), when the rotational effects of the medium are not taken into account.

In order to discuss the progress of shock wave from evolution to collapse, a particular case is considered in the next subsection.

3.3. Particular case. To improve our understanding of the flow pattern, we consider the disturbance at the boundary $r = r_0$ given by

$$\widetilde{\psi}(\zeta) = \begin{cases} 0 & \text{if } \zeta < 0, \\ Q \sin \dfrac{a_0\zeta}{r_0^{1-2\lambda}} & \text{if } 0 < \zeta < \dfrac{\pi r_0^{1-2\lambda}}{a_0},\ Q > 0, \\ 0 & \text{if } \zeta > \dfrac{\pi r_0^{1-2\lambda}}{a_0}. \end{cases} \tag{3.23}$$

From equation (3.18) we know that shock evolves on the wavelet $\zeta = 0$, which can be found out solving

$$J(r) \equiv K^* \widetilde{Q}\widetilde{\Upsilon} = 1, \tag{3.24}$$

where

$$\widetilde{Q} = \frac{Q}{\varrho_0\Omega_0^2}, \quad \widetilde{\Upsilon} = \frac{\Upsilon}{r_0^{1-3\lambda}}, \quad K^* = \frac{4\sqrt{2(1-Z_0)}\lambda^{3/2}(\Gamma+1)a_0}{\Gamma^{3/2}(1-5\lambda)\Omega_0 r_0^{\lambda}}.$$

The progress of the shock can be obtained by substituting expression (3.23) in equation (3.20) to get

$$\sin\widetilde{\zeta_2} = \frac{2\sqrt{J(r)-1}}{J(r)}, \quad \text{where } \widetilde{\zeta_2} = a_0\zeta_2/r_0^{1-2\lambda}.$$

Using equations (3.23) and (3.24), the shock formation distance for different dust parameters k_p, β, G and the parameter λ (influences the variation in the azimuthal velocity) are calculated for the cylindrical flow and are presented in Table 1. The

distortion of the pulses evolved with the variation of the dust parameters and λ are presented in Figures 1–4. For comparison, the results obtained are compared with those obtained by Chadha and Jena, for irrotational dusty, nonideal gases [2]. It is observed from Table 1 and Figures 1–4, that increase in any of the dust parameters k_p, G, β increases the shock formation distance r_s, whereas increase in λ decreases the distance where the shock is formed first.

k_p	β	G	b	λ	Γ	Irrotational dusty nonideal	Rotational dusty ideal (r_s)
0.1	0.1	10	0.0009	—	1.3939	4.7578	—
0.1	0.1	10	—	0.1	1.3939	—	4.6273
0.1	0.1	100	0.0009	—	1.3939	4.7901	—
0.1	0.1	100	—	0.1	1.3939	—	4.6273
0.1	0.5	10	0.0009	—	1.3711	4.8074	—
0.1	0.5	10	—	0.1	1.3711	—	4.9204
0.1	0.5	100	0.0009	—	1.3711	4.8397	—
0.1	0.5	100	—	0.1	1.3711	—	4.9204
0.1	0.1	10	0.0009	—	1.1939	4.7578	—
0.1	0.1	10	—	0.4	1.1939	—	1.7013
0.1	0.1	100	0.0009	—	1.1939	4.7901	—
0.1	0.1	100	—	0.4	1.1939	—	1.7013
0.1	0.5	10	0.0009	—	1.3711	4.8074	—
0.1	0.5	10	—	0.4	1.3711	—	1.7505
0.1	0.5	100	0.0009	—	1.3711	4.8397	—
0.1	0.5	100	—	0.4	1.3711	—	1.7505
0.6	0.1	10	0.0009	—	1.3306	4.6326	—
0.6	0.1	10	—	0.1	1.3306	—	5.0041
0.6	0.1	100	0.0009	—	1.3306	4.9192	—
0.6	0.1	100	—	0.1	1.3306	—	5.0041
0.6	0.5	10	0.0009	—	1.1951	4.9437	—
0.6	0.5	10	—	0.1	1.1951	—	5.0503
0.6	0.5	100	0.0009	—	1.1951	5.2578	—
0.6	0.5	100	—	0.1	1.1951	—	5.0503
0.6	0.1	10	0.0009	—	1.3306	4.6326	—
0.6	0.1	10	—	0.4	1.3306	—	1.7675
0.6	0.1	100	0.0009	—	1.3306	4.9192	—
0.6	0.1	100	—	0.4	1.3306	—	1.7675

Table 1. Comparison of shock formation distance for the rotational and irrotational (Chadha, Jena [2]) cylindrical flows of a dusty gas for varying k_p, G and β, λ.

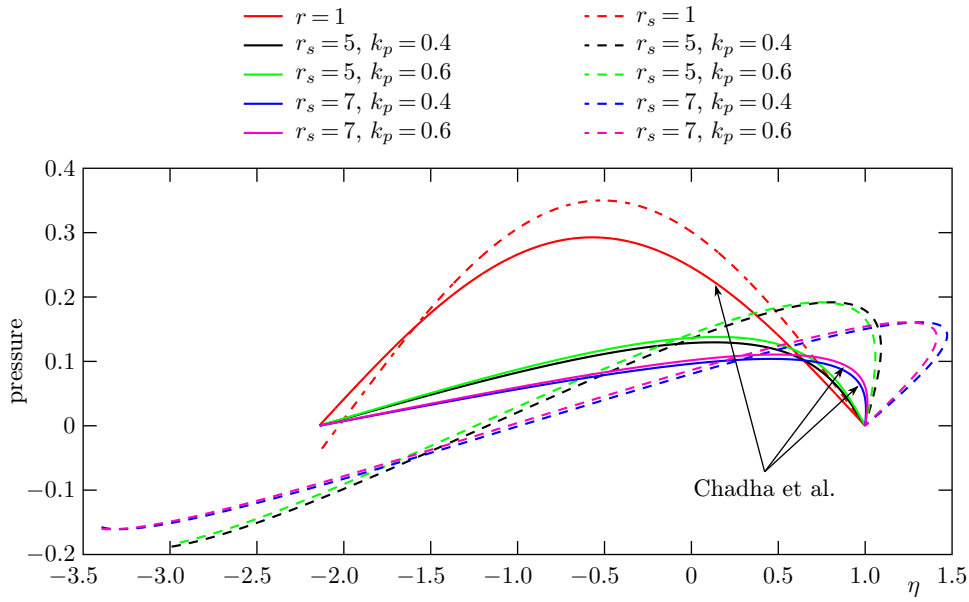

Figure 1. The distortion of the pulses with the shock formation distances for the rotational and irrotational (Chadha and Jena [2]) cylindrical flows of a dusty gas for varying k_p: $G = 1000$, $\varrho_0 = 0.1$, $\Omega_0 = 0.6$, $\beta = 0.6$, $\lambda = 0.1$, $Q = 0.1$.

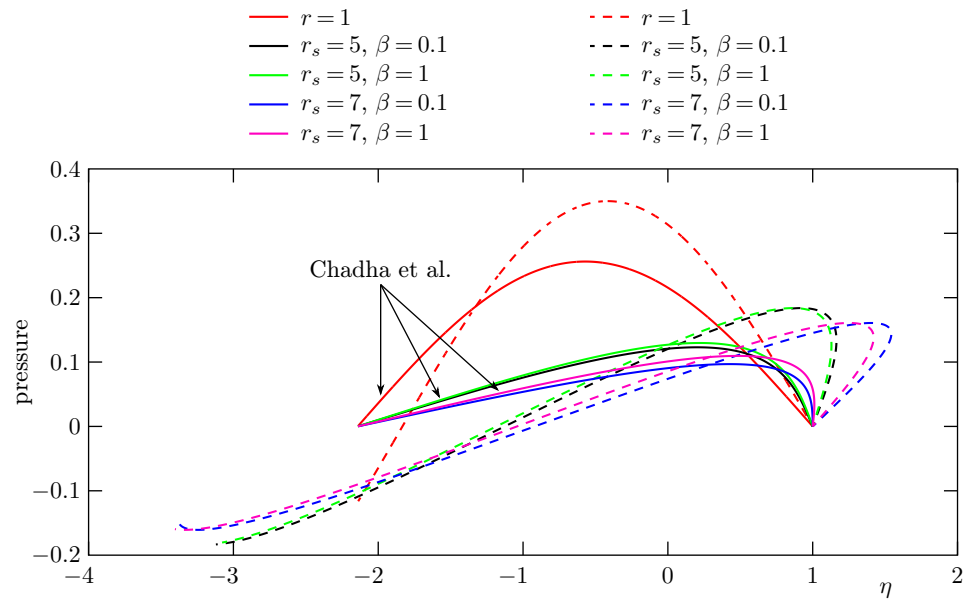

Figure 2. The distortion of the pulses with the shock formation distances for the rotational and irrotational (Chadha and Jena [2]) cylindrical flows of a dusty gas for varying β: $k_p = 0.4$, $G = 1000$, $\varrho_0 = 0.1$, $\Omega_0 = 0.6$, $\lambda = 0.1$, $Q = 0.1$.

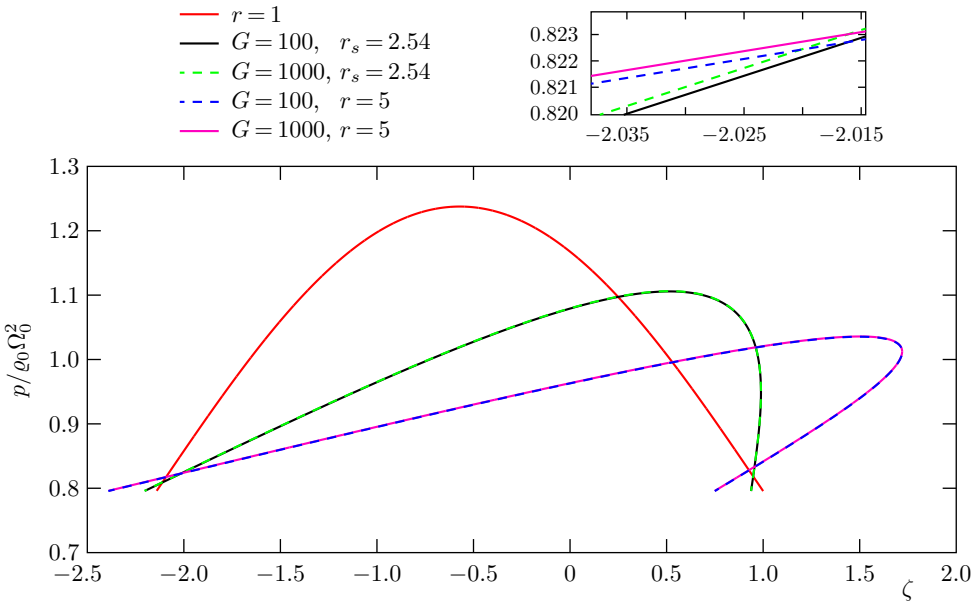

Figure 3. Distortion of the pulses with the shock formation distance with variation of G: $k_p = 0.2$, $\varrho_0 = 0.1$, $\beta = 0.6$, $\Omega_0 = 0.6$, $\lambda = 0.1$, $Q = 0.1$.

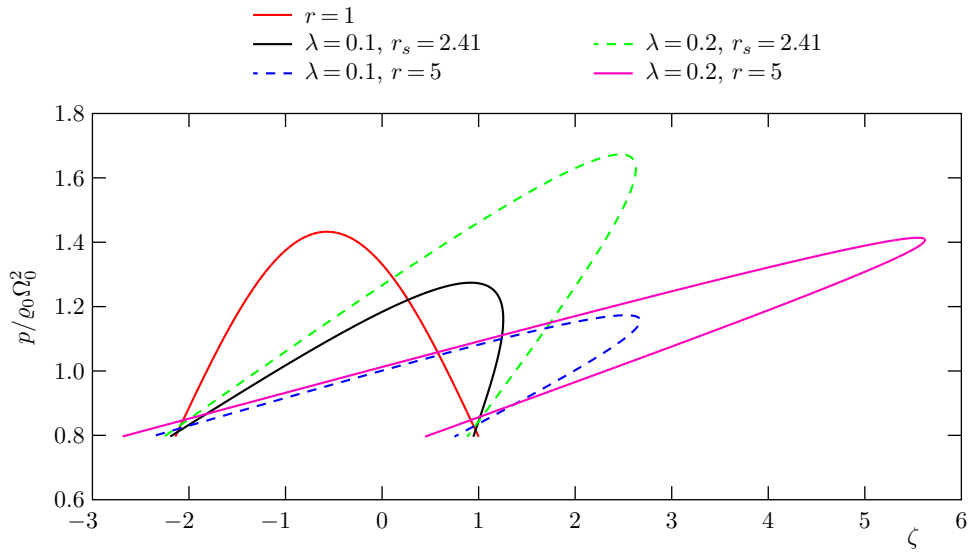

Figure 4. Distortion of the pulses with the shock formation distance with variation of λ: $k_p = 0.4$, $G = 1000$, $\varrho_0 = 0.1$, $\Omega_0 = 0.6$, $\beta = 0.6$, $Q = 0.1$.

To study the shock profile in a complete cycle $0 < \widetilde{\zeta} \leqslant 2\pi$, we assume $\widetilde{Q} < 0$, where $\widetilde{Q} = Q/(\varrho_0\Omega_0^2)$ and $\widetilde{\psi}(\zeta) = \widetilde{Q}\sin\widetilde{\zeta}_2$. Here, the shock has formed on the

wavelet $\widetilde{\zeta} = \pi$, which is situated at a distance, say $r = r^*$, ahead of r_0. Hence, the solution of equations $(3.17)_2$ and (3.19) is satisfied on the shock when the wavelets take the form $\widetilde{\zeta_1} + \widetilde{\zeta_2} = 2\pi$ and $\widetilde{\zeta_1} - \widetilde{\zeta_2} = 2\mu$, where μ is given by

$$\frac{\mu}{\sin\mu} = \frac{(\Gamma+1)\widetilde{Q}}{2(1-Z_0)}\widetilde{\Upsilon}.$$

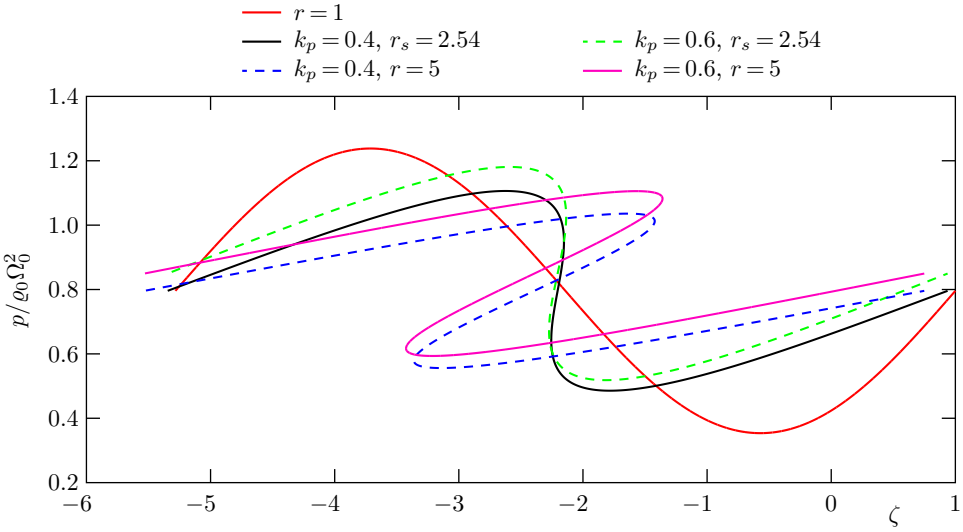

Figure 5. Distortion of the pulses with the shock formation distance influenced by dust parameter k_p: $G = 1000$, $\varrho_0 = 0.1$, $\Omega_0 = 0.6$, $\beta = 0.6$, $\lambda = 0.1$, $Q = 0.1$.

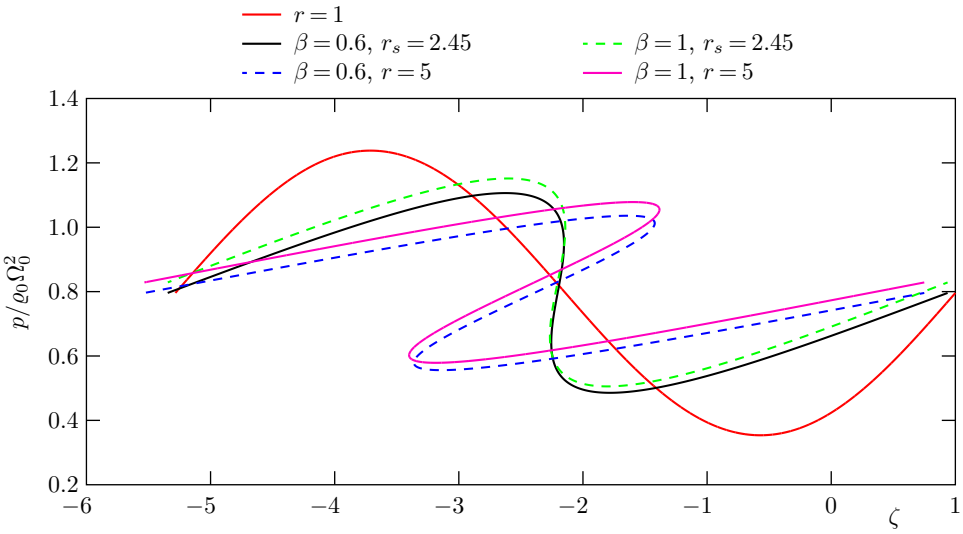

Figure 6. Distortion of the pulses with the shock formation distance influenced by dust parameter β: $G = 1000$, $\varrho_0 = 0.1$, $\Omega_0 = 0.6$, $k_p = 0.4$, $\lambda = 0.1$, $Q = 0.1$.

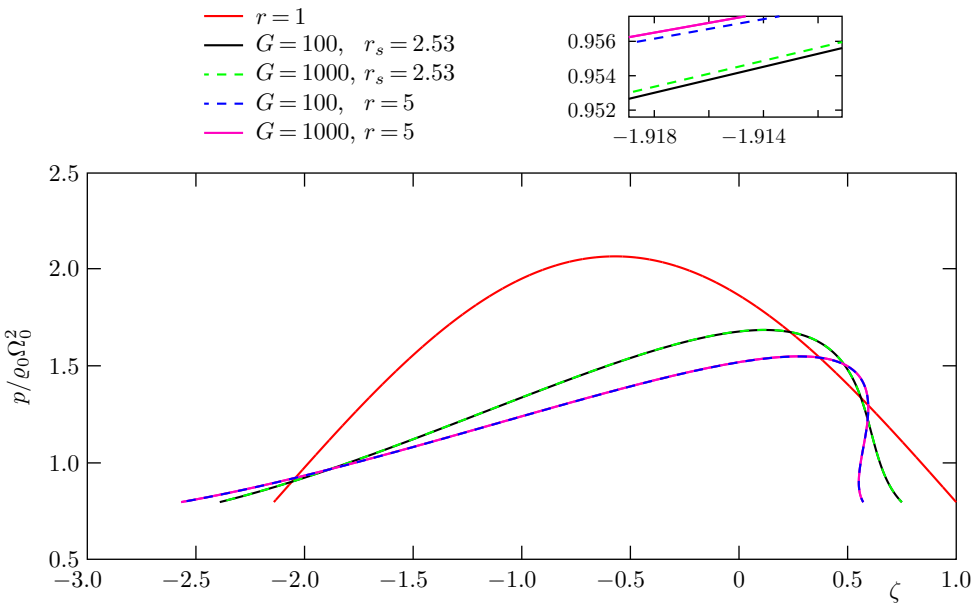

Figure 7. Distortion of the pulses with the shock formation distance influenced by dust parameter G: $k_p = 0.2$, $\varrho_0 = 0.1$, $\beta = 0.6$, $\Omega_0 = 0.6$, $\lambda = 0.1$, $Q = 0.1$.

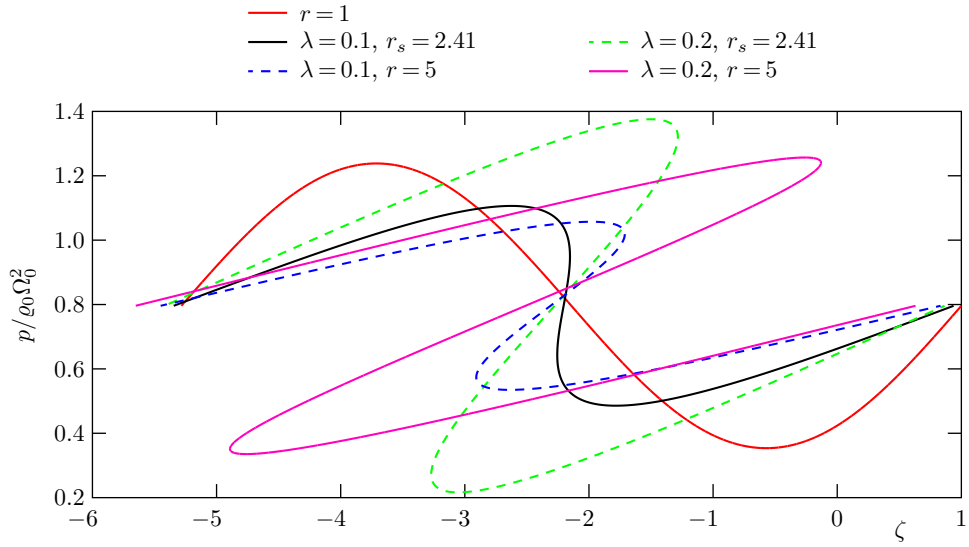

Figure 8. Distortion of the pulses with the shock formation distance influenced by λ: $G = 1000$, $\varrho_0 = 0.1$, $\Omega_0 = 0.6$, $\beta = 0.6$, $k_p = 0.4$, $Q = 0.1$.

In Figures 5–8, the wave profiles for complete cycle are depicted for different values of k_p, β, G and λ.

4. The waves with amplitude not so small

In this section we involve the quadratic terms in the perturbed flow variables p, ϱ etc., which were ignored earlier. Equation (3.12) on including the quadratic terms become

$$2\frac{\partial p^{(1)}}{\partial r} + \frac{(1-\lambda)}{2}\frac{p^{(1)}}{r} + \frac{(p^{(1)})^2}{8\Gamma p_0 r}\mu_* = 0, \tag{4.1}$$

$$\frac{\partial \tau}{\partial r} = \frac{1}{a_0}\Big\{1 - \frac{(\Gamma+1)}{2\Gamma}\frac{p^{(1)}}{p_0} + \frac{(\Gamma+1)}{8\Gamma^2}(3(\Gamma+1) - 2Z_0)\Big(\frac{p^{(1)}}{p_0}\Big)^2\Big\}, \tag{4.2}$$

where

$$\mu_* = \Big((\Gamma+1)\lambda + \frac{(\Gamma - 3 + 4Z_0)}{4\Gamma} - 8\Gamma\lambda f(\Gamma)\Big),$$
$$f(\Gamma) = (3(\Gamma+1) - 2Z_0) - \frac{(3\Gamma^2 + 2\Gamma + 1)}{8\Gamma^2}.$$

Solving equations (4.1) and (4.2) using the boundary conditions (3.10), $p^{(1)}$ and τ take the form

$$p^{(1)} = \widetilde{\psi}(\zeta)\Big(\frac{r}{r_0}\Big)^{-(1-\lambda)/2}\Big\{1 + \widetilde{\psi}(\zeta)\frac{r_0^{-2\lambda}}{\alpha}\mu_*\Big(\Big(\frac{r}{r_0}\Big)^{-(1+3\lambda)/2} - 1\Big)\Big\}^{-1}, \tag{4.3}$$

$$K_1(\tau - \zeta) = \Big\{(r - r_0)^{-\lambda+1} - \frac{(\Gamma+1)}{2\Gamma}\int_{r_0}^{r} r^{-\lambda}\frac{p^{(1)}}{p_0}\,\mathrm{d}r + R_1\int_{r_0}^{r} r^{-\lambda}\Big(\frac{p^{(1)}}{p_0}\Big)^2\Big\},$$

where

$$R_1 = \frac{(\Gamma+1)(3(\Gamma+1) - 2Z_0)}{8\Gamma^2}.$$

Pfriem's rule suggests that the shock velocity of a weak shock is the average of the characteristic speeds behind and ahead the shock. Accordingly, if $(\mathrm{d}\tau/\mathrm{d}r)\,|_s$ is the shock velocity, then at any position $p^{(1)} = p^{(1)}(r, \zeta_s)$, it is given by

$$\frac{\mathrm{d}\tau}{\mathrm{d}r}\Big|_s = \frac{1}{a_0}\Big\{1 - \frac{\lambda(\Gamma+1)}{r^{2\lambda}\Gamma}\frac{p^{(1)}}{\varrho_0\Omega_0^2} + 4\lambda^2 R_1\frac{{p^{(1)}}^2}{r^{4\lambda}\varrho_0^2\Omega_0^4}\Big\}. \tag{4.4}$$

The above expression for shock speed also has an alternative approach and is given by

$$\frac{\mathrm{d}\tau}{\mathrm{d}r}\Big|_s = \frac{1}{a_0}\frac{\mathrm{d}\zeta_s}{\mathrm{d}r}\Big\{1 - \frac{\Gamma+1}{2\Gamma}\int_{r_0}^{r} r^{-\lambda}\frac{\partial_\zeta p^{(1)}}{p_0}\,\mathrm{d}r + R_1\int_{r_0}^{r} r^{-\lambda}\frac{2p_1\partial_\zeta p^{(1)}}{p_0^2}\,\mathrm{d}r\Big\} \tag{4.5}$$
$$+ \frac{1}{a_0}\Big\{1 - \frac{\lambda(\Gamma+1)}{r^{2\lambda}\Gamma}\frac{p^{(1)}}{\varrho_0\Omega_0^2} + 4\lambda^2 R_1\frac{{p^{(1)}}^2}{r^{4\lambda}\varrho_0^2\Omega_0^4}\Big\}.$$

Elimination of $\mathrm{d}\tau/\mathrm{d}r$ from equations (4.1) and (4.2) leads to a differential equation in ζ_s, which on solving numerically leads to evaluation of the shock strength for

different locations. The results are depicted in Figures 9–12. It is observed that on increasing any of the dust parameters k_p, β, G and λ, the onset of the shock formation gets delayed, i.e., the shock formation distance increases.

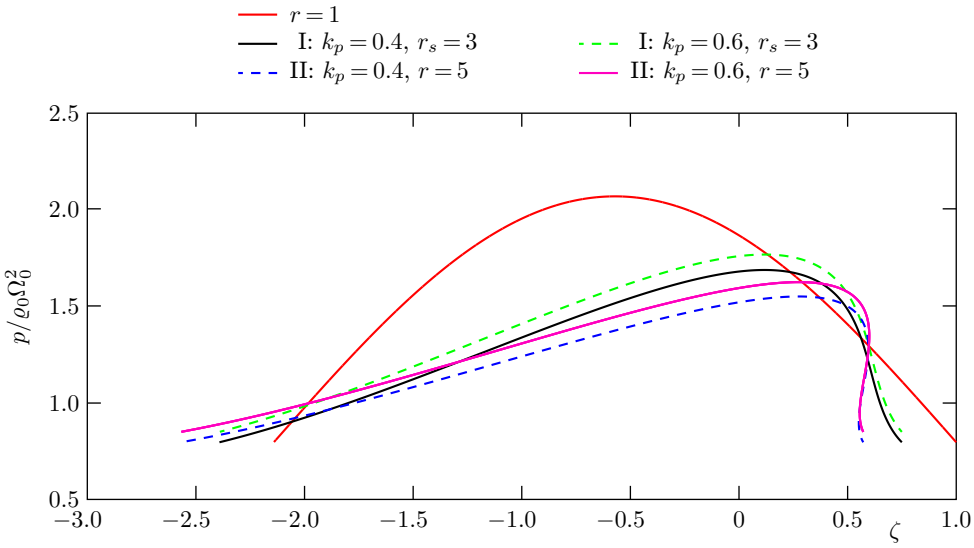

Figure 9. Distortion of large amplitude pulses with the shock formation distance influenced by k_p: $G = 1000$, $\varrho_0 = 0.1$, $\Omega_0 = 0.6$, $\beta = 0.6$, $\lambda = 0.1$, $Q = 0.1$.

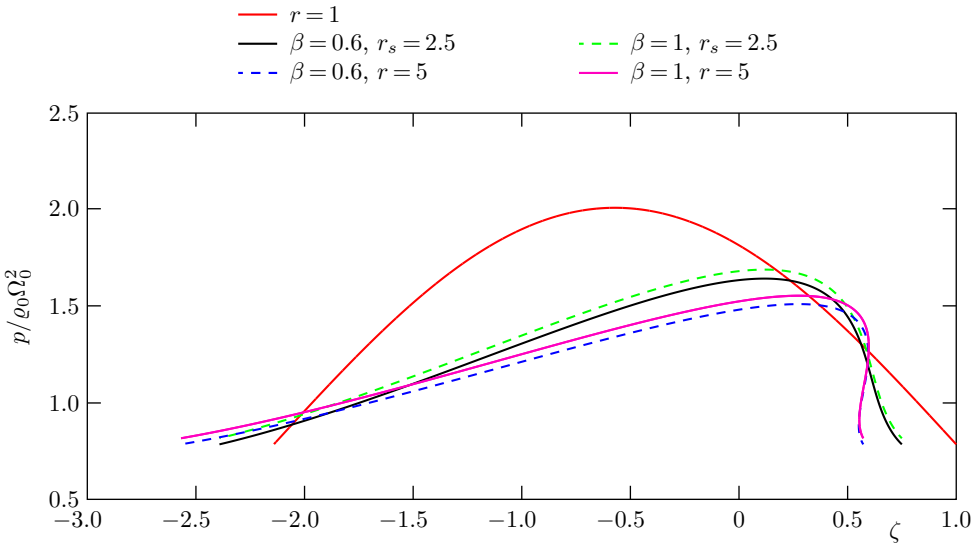

Figure 10. Distortion of large amplitude pulses with the shock formation distance influenced by β: $G = 1000$, $\varrho_0 = 0.1$, $\Omega_0 = 0.6$, $k_p = 0.4$, $\lambda = 0.1$, $Q = 0.1$.

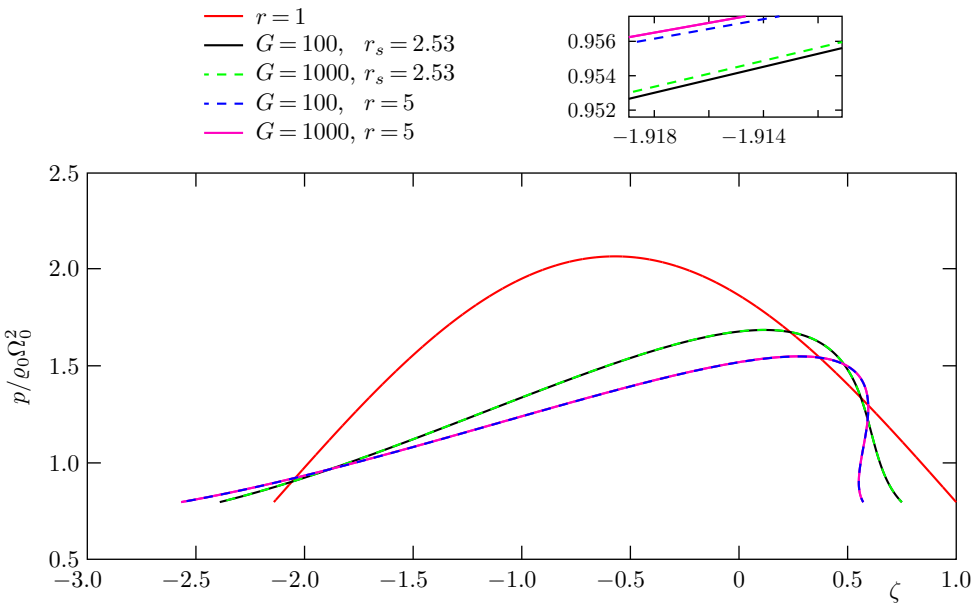

Figure 11. Distortion of large amplitude pulses with the shock formation distance influenced by G: $k_p = 0.2$, $\varrho_0 = 0.1$, $\beta = 0.6$, $\Omega_0 = 0.6$, $\lambda = 0.1$, $Q = 0.1$.

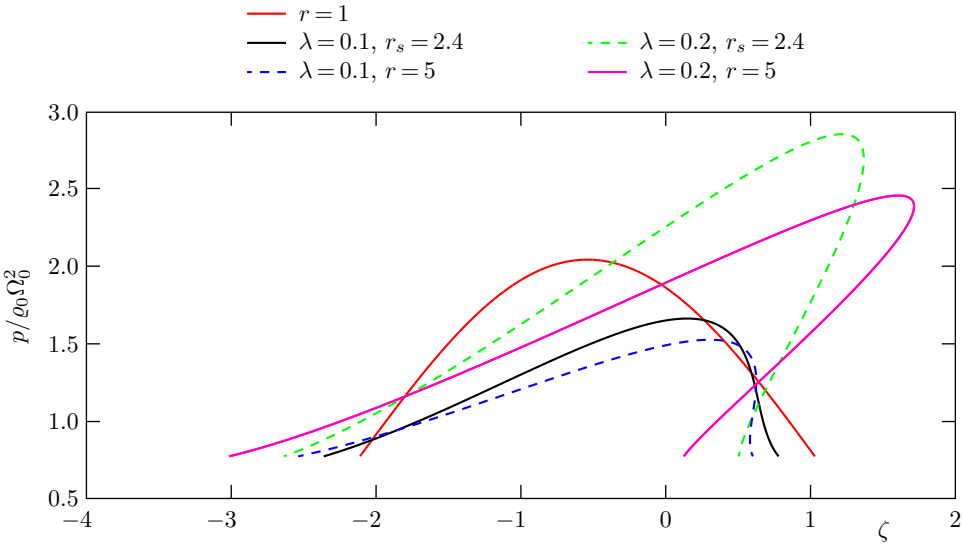

Figure 12. Distortion of large amplitude pulses with the shock formation distance influenced by λ: $G = 1000$, $\varrho_0 = 0.1$, $\Omega_0 = 0.6$, $\beta = 0.6$, $k_p = 0.4$, $Q = 0.1$.

5. Asymptotic expansion

In this section, the results obtained in the previous section are compared and the study of the behaviour of the flow is extended to nonlinear geometrical acoustic solutions. The asymptotic analysis is used to discuss the small-amplitude wave like disturbances governed by the system of equations (2.1) in the high frequency time limit using the series expansion method. If the characteristic time scale of the medium t_2, is very large as compared to the time scale at the boundary t_1, then we introduce ε such that $\varepsilon = t_1/t_2 \ll 1$, see [5]. In this scale the disturbances of the flow variables are of size $O(\varepsilon)$ and they mainly depend on the fast characteristic variable $\eta = \zeta/\varepsilon$. In order to investigate the nonlinearity, we change the independent variables from (r,t) to (r,η) by characterising $r = r$ and $t = \widetilde{\tau}(r,\eta)$. The asymptotic expansions for flow variables take the form

$$\begin{aligned} \widetilde{U}(r,\eta) &= U^{(0)} + \varepsilon U^{(1)}(r,\eta) + \varepsilon^2 U^{(2)}(r,\eta) + O(\varepsilon^2), \\ \widetilde{\tau}(r,\eta) &= \tau^{(0)} + \varepsilon \tau^{(1)}(r,\eta) + \varepsilon^2 \tau^{(2)}(r,\eta) + O(\varepsilon^2), \end{aligned} \tag{5.1}$$

subject to the boundary condition given by (3.10)

$$p(r_0,\eta) = p_0 + \varepsilon\psi(\eta), \quad \widetilde{\tau} = \varepsilon\eta. \tag{5.2}$$

Here, $U^{(0)}$ indicates the uniform reference state of the flow variables. Using the expansion (5.1) in equations (2.1) and equating the coefficients of various powers of ε (up to the second order), the following set of equations is obtained:

$$\begin{aligned}
\underline{O(1)}\colon\quad & \tau^{(0)} = \frac{r-r_0}{a_0} = 0, \quad \frac{\partial \tau^{(0)}}{\partial r} = \frac{1}{a_0}. \\
\underline{O(\varepsilon)}\colon\quad & \varrho_\eta^{(1)} = \frac{\varrho_0}{a_0} u_\eta^{(1)}, \quad u_\eta^{(1)} = \frac{1}{a_0\varrho_0} p_\eta^{(1)}, \quad v_\eta^{(1)} = 0, \\
& p_r^{(1)} = -\frac{p^{(1)}}{2r}(1-\lambda), \quad \tau_r^{(1)} = (u^{(1)} + a^{(1)})^{-1}. \\
\underline{O(\varepsilon^2)}\colon\quad & \varrho_\eta^{(2)} = \frac{1}{a_0^2}\Big\{ p_\eta^{(2)} + \tau_\eta^{(1)}\Big(\frac{a_0}{r}(\varrho^{(1)} v_0^2 + 2\varrho_0 v_0 v^{(1)}) \\
& \qquad\qquad - \frac{a_0^2\varrho_0}{r}\Big(u^{(1)} + \frac{u^{(1)}}{r}\Big) - a_0 p_r^{(1)}\Big)\Big\}, \\
& u_\eta^{(2)} = \frac{1}{a_0\varrho_0}\Big\{ p_\eta^{(2)} + a_0\tau_\eta^{(1)}\Big(\frac{\varrho^{(1)} v_0^2}{r} + \frac{2\varrho_0 v_0^2}{r} - p_r^{(1)}\Big) \\
& \qquad\qquad - a^{(1)}\varrho_0 u_\eta^{(1)} - a_0\varrho^{(1)} u_\eta^{(1)}\Big\},
\end{aligned}$$

and

$$v_\eta^{(2)} = -\tau_\eta^{(1)} u^{(1)}\Big(v_{0_r} + \frac{v_0}{r}\Big). \tag{5.3}$$

The transport equations obtained are given by

(5.4)

$$p_r^{(2)} + \frac{A_1}{2r}p^2 - \frac{r^{-(5-3\lambda)/2}}{2r_0^{-(1-\lambda)/2}}\Big\{A_2\Big(I - \frac{K_3\Upsilon\psi^2}{2}\Big) + (\eta - K_3\Upsilon\psi)A_3\Big\}$$
$$- \frac{A_4\psi^2 r^{-(\lambda+2)}}{4r_0^{\lambda-1}} - A_5(\eta - K_3\Upsilon\psi) - \frac{A_6 r^{-2}}{r_0^{-(1-\lambda)}} - A_7\frac{r^{-(3-\lambda)/2}}{r_0^{-(1-\lambda)/2}} - A_8\frac{r^{-(2-\lambda)}}{r_0^{-(1-\lambda)}} = 0,$$
$$\tau_r^{(2)} = \frac{1}{a_0^3}(u_1 + a_1)^2 - \frac{1}{a_0^2}(u^2 + a^2),$$

where

$$A_1 = \frac{(\lambda+1)\Gamma - \lambda(1-2\theta\varrho_0)}{\Gamma}, \quad A_2 = K_{11}^3\frac{1}{(1-Z_0)},$$
$$A_3 = \frac{k_{11}}{2}\Big\{k_{11}^2 + \frac{1}{k_{11}^2} + \frac{3(\lambda-1)}{2} - \frac{3(\lambda-1)^2}{4} - 1\Big\},$$
$$A_4 = \frac{1}{4}\Big\{1 + K_{11}^{-2} + K_{11}^{-1/2}\frac{(\lambda-1)(\Gamma+1)}{4\lambda\Gamma} - \sqrt{2}(1-5\lambda)(\Gamma+1)k_{11}^{-1/2}$$
$$- \frac{4\lambda^2 Z_0(\Gamma - 1 + 2Z_0)}{\Gamma^2(1-Z_0)} + \frac{1}{2\lambda}(\lambda(\Gamma - 1 + 2Z_0)(1+3\lambda))\Big\},$$
$$A_5 = \frac{\lambda(1-2Z_0)}{4\sqrt{\Gamma(1-Z_0)}}K_{11}^3, \quad A_6 = \frac{(\Gamma - 1 + 2Z_0)}{2\Gamma}(1 + 2K_{11}^{-1}),$$
$$A_7 = \{K_{11}^{-1} - K_{11}(1-5\lambda)(\Gamma+1)\sqrt{2}\Gamma^{-3/2}\},$$
$$A_8 = \frac{\lambda(\Gamma - 1 + 2Z_0)(1-2Z_0)}{2\Gamma(1-Z_0)}, \quad K_{11} = \Big(\frac{\Gamma}{2\lambda(1-Z_0)}\Big)^{1/2}.$$

Solving equations (5.3) and (5.4) leads to the following results:

(5.5)

$$\varrho^{(1)} = \frac{\varrho_0}{a_0}u^{(1)}, \quad u^{(1)} = \frac{p^{(1)}}{a_0\varrho_0}, \quad v^{(1)} = f(r),$$
$$p^{(1)} = \psi(\eta)X^{-(1-\lambda)/2}, \quad \tau^{(1)} = \eta - \psi(\eta)K_1^{-1}K_2\Upsilon,$$
$$\varrho^{(2)} = \Big\{\frac{p^{(2)}}{a_0^2} + \frac{2\varrho_0\Omega_0^2}{K_1}r^{-(1-\lambda)}(\eta - K_3\Upsilon\psi(\eta)) + \frac{\Omega_0^2(I - (K_3\Upsilon\psi(\eta)^2/2))}{K_1^3 r_0^{-(1-\lambda)/2}}r^{-(\lambda+3)/2}$$
$$+ \frac{K_1^2\lambda\psi^2(\gamma - 1 + 2\theta\varrho_0)}{\Gamma\varrho_0 r_0^{-(1-\lambda)}}r^{-(2-3\lambda)}\Big\},$$
$$u^{(2)} = \frac{1}{a_0\varrho_0}\Big\{p^{(2)} + (\eta - K_3\Upsilon\psi(\eta))$$
$$\times\Big(\frac{(\Omega_0^2 - K_1^2\lambda + K_1)}{2K_1 r_0^{-(1-\lambda)/2}}\psi r^{-3(1-\lambda)/2} + 2\varrho_0 K_1\Omega_0^2 r^{-(1-3\lambda)}\Big)$$
$$- \frac{(\Gamma - 1 + 2\theta\varrho_0)\psi(\eta)^2}{2K_1^2\varrho_0(1-\theta\varrho_0)r_0^{-(1-\lambda)}}r^{-1} - \frac{\psi(\eta)^2}{2K_1^2\varrho_0 r_0^{-(1-\lambda)}}r^{-(1-\lambda)}\Big\},$$

where $X = (r/r_0)$ and Υ is given by equation (3.21). Solving equations (5.4_1) and (5.4_2) yield the following second order solutions for $p^{(2)}$ and $\tau^{(2)}$:

(5.6)
$$p^{(2)} = T_1(X^{-3(1-\lambda)/2} - 1) + T_2(X^{-(1+\lambda)} - 1) + T_3(X^{-(1-3\lambda)} - 1) + T_4(X^{(1-\lambda)/2} - 1) + T_5(X - 1) + T_6(X^{-(\lambda-1)/2} - 1) + T_7(X^{-(1-\lambda)} - 1),$$

with

$$T_1 = R_1 r_0^{1-\lambda} + R_2 r_0^{-2\lambda} + R_3 r_0^{1-2\lambda}, \quad T_2 = R_4 r_0^{-2\lambda} + R_5^{(1-9\lambda)/2},$$
$$T_3 = \frac{2\varrho_0\Omega_0^3 A_5}{(2-6\lambda-A_1)}(\zeta r_0^{-(1-3\lambda)} + K_3\psi(\eta)), \quad T_4 = 2\varrho_0\Omega_0^3 A_5 K_3\psi(\eta),$$
$$T_5 = \frac{\psi(\eta)^2 A_6}{\varrho_0\Omega_0^2} r_0^{-\lambda}, \quad T_6 = -\frac{2\psi(\eta)A_7}{(1-\lambda)}, \quad T_7 = -T_6,$$
$$R_1 = \frac{4\Omega_0 I}{3(2-2\lambda-A_1)}(A_3 - A_2), \quad R_2 = \frac{2K_3\psi(\eta)^2\Omega_0 A_2}{3(2-2\lambda-A_1)}, \quad R_3 = \frac{-K_3\psi(\eta)^2\Omega_0 A_2}{(2+2\lambda+A_1)},$$
$$R_4 = \frac{\psi(\eta)^2}{(2+2\lambda+A_1)}(A_4 - K_3 A_2\Omega_0), \quad R_5 = \frac{\psi(\eta)^2 A_4}{\varrho_0\Omega_0^2(2+2\lambda+A_1)},$$

and

(5.7)
$$\tau^{(2)} = S_1(X^{-(1+3\lambda)/2} - 1) + S_2(X^{1-3\lambda} - 1) + S_3(X^{-4\lambda} - 1) + S_4(\ln X - 1) + S_5(X^{(3-5\lambda)/2} - 1) + S_6(X^{2-3\lambda} - 1) + S_7(X^{(1-5\lambda)/2} - 1) + S_8(X^{-2\lambda} - 1) + S_9 t(X^{3\lambda} - 1) + S_{10}(X^{1-5\lambda} - 1) + S_{11}(X^{(1-9\lambda)/2} - 1) + S_{12}(X^{3(1+\lambda)/2} - 1) + S_{13}(X^{-(1-2\lambda)} - 1),$$

with

$$S_1 = \frac{\psi(\eta) r_0^{-2\lambda}}{\varrho_0 K_{11}^2\Omega_0^2}\Big(\frac{\eta}{K_{11}^2} - \frac{r_0(1-\lambda)}{2}\Big) + \frac{\psi(\eta)^2 K_3}{\varrho_0\Omega_0^2 K_{11}^4} r_0^{1-5\lambda} - \frac{2TT_1 r_0^{1-3\lambda}}{(1+3\lambda)},$$
$$S_2 = -\frac{Tr_0^{1-3\lambda}}{1-3\lambda}\Big(T_1 + T_2 + T_3 + \frac{\psi(\eta)^2 A_6}{\varrho_0\Omega_0^2} - r_0^{-(1-2\lambda)}\frac{2\psi(\eta)A_7}{1-\lambda} + \frac{\psi(\eta)^2 A_8}{\varrho_0\Omega_0^2(1-\lambda)}\Big),$$
$$S_3 = \frac{T\psi(\eta)^2}{2+2\lambda+A_1}\Big(\frac{A_4}{\varrho_0\Omega_0^2} - K_3 A_2\Omega_0\Big), \quad T = \frac{\Gamma + Z_0}{K_{11}\varrho_0\Omega_0^3(1-Z_0)},$$
$$S_4 = \frac{2}{K_{11}^2} - \frac{2A_5\Gamma + Z_0}{K_{11}(1-Z_0)(2-6\lambda-A_1)}(K_3\psi(\eta)r_0^{-(1-3\lambda)} - \eta),$$
$$S_5 = -\frac{2\psi(\eta)^2 A_8(\Gamma+Z_0)r_0^{1-2\lambda}}{K_{11}\varrho_0\Omega_0^3(1-Z_0(3-5\lambda))}, \quad S_6 = -\frac{(\Gamma+Z_0)A_5\eta r_0^{-\lambda}}{(1-Z_0)K_{11}(1-3\lambda)},$$
$$S_7 = -\frac{2(\Gamma+Z_0)A_5\eta r^{-\lambda}}{(1-Z_0)K_{11}(1-3\lambda)},$$
$$S_8 = -\frac{(\Gamma+Z_0)A_5 K_3\psi(\eta)}{2\lambda K_{11}(1-Z_0)} r^{1-3\lambda} + \frac{1-2Z_0}{(1-Z_0)K_{11}^4\Omega_0^2}\Big(\frac{\eta r_0^{-2\lambda}}{2\lambda} + K_3\psi(\eta)r_0^{1-5\lambda}\Big),$$

$$S_9 = \frac{\Gamma - 1 + 2Z_0}{6K_{11}^5 \varrho_0^2 \Omega_0^4}\Big(\frac{1}{3\Omega_0(1-Z_0)} + \frac{(1-2Z_0)\psi(\eta)^2 r_0^{1-4\lambda}}{4(1-Z_0)^2}\Big), \quad S_{10} = -\frac{\psi(\eta)^2}{8\lambda K_{11}^5 \varrho_0^2 \Omega_0^5},$$

$$S_{11} = \frac{r_0^{1-5\lambda}\psi(\eta)}{(1-Z_0)K_{11}^4\Omega_0^2}\Big\{\frac{2(1-2Z_0)K_3}{1-9\lambda} + \frac{\psi(\eta)}{8\Omega_0^3 K_{11}\varrho_0(1-Z_0)}((\Gamma-1+2Z_0)^2 + 8Z_0)\Big\},$$

$$S_{12} = \frac{(1-2Z_0)\psi(\eta)^3 r_0^{1-2\lambda}}{\varrho_0 K_{11}^4(1-Z_0)}, \quad S_{13} = -\frac{(\Gamma-1+2Z_0)(1-2Z_0)K_{11}\lambda\Omega_0^2\psi(\eta)r_0^\lambda}{2\Gamma\varrho_0(1-Z_0)(1-2\lambda)}.$$

The first order solutions obtained in the previous section, i.e., $p^{(1)}$ and $\tau^{(1)}$ given by (3.17), agree with the solutions obtained from equation (5.5). However, the second order solutions, $p^{(2)}$ and $\tau^{(2)}$, depend upon the precursor wavelets. The nonlinear distortion profiles up to the second order for various values of k_p, β and λ are depicted in Figures 13–15.

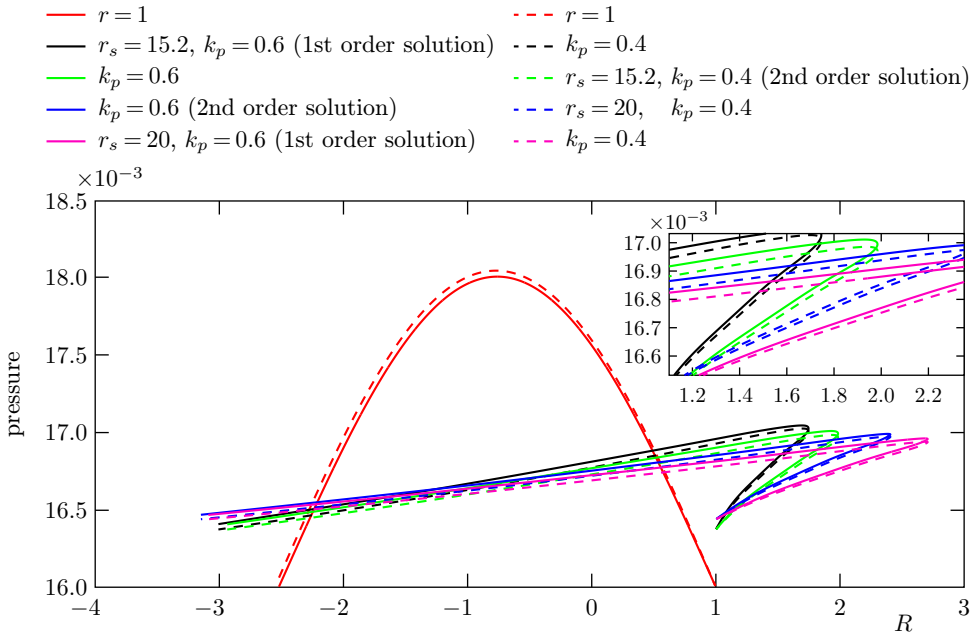

Figure 13. Distortion of the pulses with the shock formation distance influenced by dust parameters with varying k_p, $G = 1000$, $\varrho_0 = 0.1$, $\Omega_0 = 0.6$, $\beta = 0.6$, $\lambda = 0.1$, $Q = 0.1$.

It is evident from Figures 13 and 14 that as k_p and β increase, the pressure in the waves increases initially and then decays much faster as compared to waves with lesser values of dust parameters. The results with variation of dust parameter G were found to be similar. For higher values of λ, the pressure is higher and the wavelets decay faster as compared to wavelets with lower values (Figure 15).

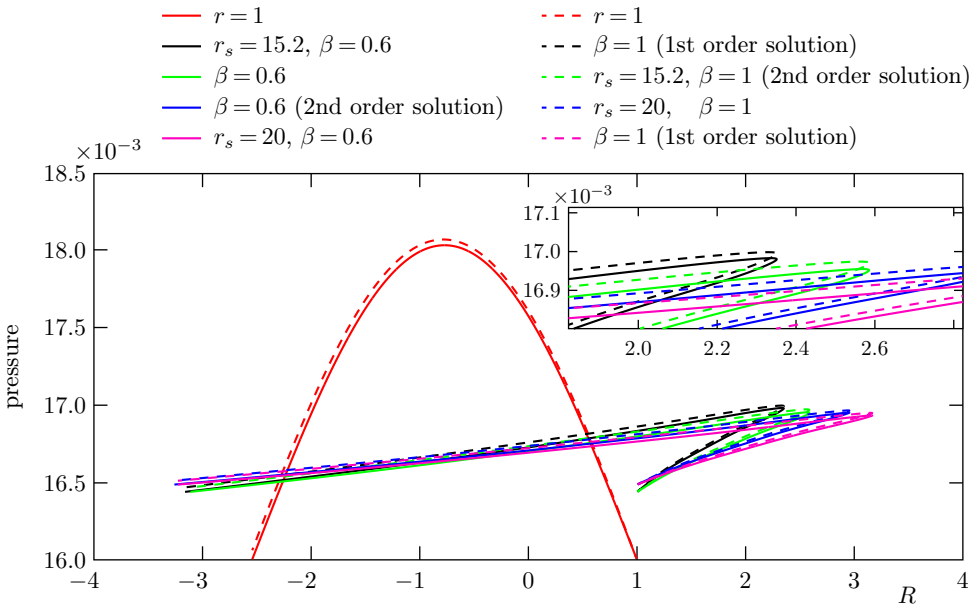

Figure 14. Distortion of the pulses with the shock formation distance influenced by dust parameters with varying β, $G = 1000$, $\varrho_0 = 0.1$, $\Omega_0 = 0.6$, $k_p = 0.4$, $\lambda = 0.1$, $Q = 0.1$.

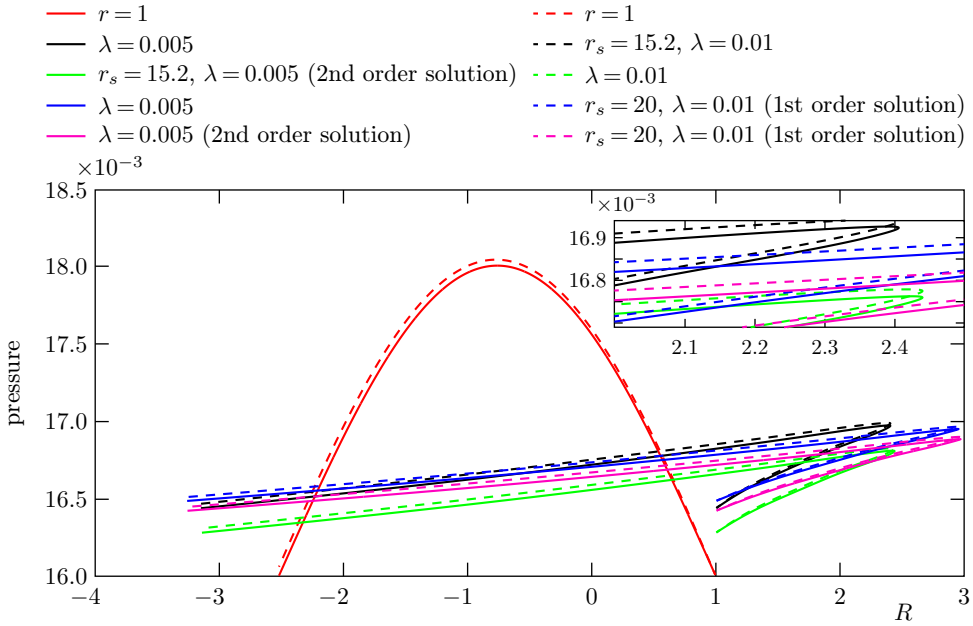

Figure 15. Distortion of the pulses with the shock formation distance influenced by varying rotational parameter λ, $k_p = 0.4$ $G = 1000$, $\varrho_0 = 0.1$, $\Omega_0 = 0.6$, $\beta = 0.6$, $Q = 0.1$.

6. Conclusion

The present work discusses the one-dimensional unsteady cylindrical flow of pseudo-fluid undergoing rotational effects with constant angular velocity and variable azimuthal velocity. The study is broadly categorised into two parts. In the first part, the theory of relatively undistorted waves is used to study the shock formation distance and the results are compared using the asymptotic expansion in the second part. The solutions obtained by both methods are in accordance with each other. The small and large amplitude pulses are analysed and results are presented in Figures 1–12.

The shock formation distance for different values of dust parameters k_p, β, G and the parameter λ, which influences the azimuthal velocity, are presented in Table 1. For comparison the shock formation distance for rotational dusty gases have been compared to the shock formation distance in an irrotational, dusty, nonideal gas [2] (Table 1 and Figures 1 and 2).

The results show significant variations in the flow field due to the presence of dust particles and rotation with constant angular velocity Ω_0. It is observed from Figures 4, 8, 12, 15 and Table 1 that as λ increases, the pressure in the waves increases and the distance where the shock is formed first decreases. The distortion of the propagating disturbance shows that for higher values of the variable λ, enhanced decay in the shock formation distance is observed which results in a steepness of the pulse. In other words, in a rotational flow, the higher the values of λ the more steepening in the pulses; the same was observed by [7]. It is also observed that although the pressure in the wavelets is higher initially for higher values of dust parameters, the wavelets decay much faster when compared to the waves with smaller values of dust parameters.

The relation $v = \Omega_0 r^\lambda$ for constant angular velocity Ω_0 and $\lambda < 1$ implies that as the radial distance increases, the azimuthal velocity increases for a particular value of λ and vice versa. When the azimuthal velocity decreases, the energy created by the rotational effects slows down adding inertia to the medium. This causes an enhancement in the decay of the distortion. An increase in the dust parameter k_p means that the volumetric fraction of the dust particles present in the mixture reduces the compressibility of the mixture. The reduced compressibility influences the inertia of the mixture, which enhances the decaying of the shock wave [3].

References

[1] *R. K. Anand*: Shock jump relations for a dusty gas atmosphere. Astrophys. Space Sci. *349* (2014), 181–195. doi

[2] *M. Chadha, J. Jena*: Propagation of weak waves in a dusty, van der Waals gas. Meccanica *51* (2016), 2145–2157. zbl MR doi

[3] *M. Chadha, J. Jena*: Impact of dust in the decay of blast waves produced by a nuclear explosion. Proc. R. Soc. Lond., A, Math. Phys. Eng. Sci. *476* (2020), Article ID 20200105, 22 pages. zbl MR doi
[4] *P. Chaturani*: Strong cylindrical shocks in a rotating gas. Appl. Sci. Res. *23* (1971), 197–211. zbl doi
[5] *J. Jena, V. D. Sharma*: Propagation and interaction of waves in a non-ideal gas. ZAMM, Z. Angew. Math. Mech. *81* (2001), 417–429. zbl doi
[6] *V. A. Levin, G. A. Skopina*: Detonation wave propagation in rotational gas flows. J. App. Mech. Tech. Phys. *45* (2004), 457–460; translated from Prikl. Mekh. Tekh. Fiz. *45* (2004), 3–6. zbl doi
[7] *G. Nath*: Self-similar solutions for unsteady flow behind an exponential shock in an axisymmetric rotating dusty gas. Shock Waves *24* (2014), 415–428. doi
[8] *G. Nath, P. K. Sahu, S. Chaurasia*: Self-similar solution for the flow behind an exponential shock wave in a rotational axisymmetric non-ideal gas with magnetic field. Chinese J. Phys. *58* (2019), 280–293. doi
[9] *S. I. Pai*: Two Phase Flows. Vieweg Tracts in Pure and Applied Physics 3. Vieweg, Braunschweig, 1977. zbl MR doi
[10] *N. D. Palo, J. Jena, M. Chadha*: An analytical approach to study kinematics of shock waves in a dusty, cylindrical gas flow. ZAMM, Z. Angew. Math. Mech. *102* (2022), Article ID e202200019, 20 pages. MR doi
[11] *D. F. Parker, B. R. Seymour*: Finite amplitude one-dimensional pulses in an inhomogeneous granular material. Arch. Ration. Mech. Anal. *72* (1980), 265–284. zbl MR doi
[12] *C. Radha, V. D. Sharma*: Propagation and interaction of waves in a relaxing gas. Philos. Trans. R. Soc. Lond., Ser. A *352* (1995), 169–195. zbl doi
[13] *P. K. Sahu*: Propagation of an exponential shock wave in a rotational axisymmetric isothermal or adiabatic flow of a self-gravitating non-ideal gas under the influence of axial or azimuthal magnetic field. Chaos Solitons Fractals *135* (2020), Article ID 109739, 22 pages. zbl MR doi
[14] *E. Varley, E. Cumberbatch*: Non-linear, high frequency sound waves. J. Inst. Math. Appl. *2* (1966), Article ID 133–143. zbl doi
[15] *E. Varley, E. Cumberbatch*: Large amplitude waves in stratified media: Acoustic pulses. J. Fluid Mech. *43* (1970), 513–537. zbl MR doi
[16] *J. P. Vishwakarma, G. Nath*: Propagation of a cylindrical shock wave in a rotating dusty gas with heat conduction and radiation heat flux. Phys. Scr. *81* (2010), Article ID 045401, 9 pages. zbl doi
[17] *J. P. Vishwakarma, G. Nath*: Similarity solution for a cylindrical shock wave in a rotational axisymmetric dusty gas with heat conduction and radiation heat flux. Commun. Nonlinear Sci. Numer. Simul. *17* (2012), 154–169. zbl MR doi
[18] *G. B. Whitham*: On the propagation of weak shock waves. J. Fluid Mech. *1* (1956), 290–318. zbl MR doi
[19] *G. B. Whitham*: Linear and Nonlinear Waves. Pure and Applied Mathematics. John Wiley & Sons, New York, 1974. zbl MR doi

Authors' addresses: *Nishi Deepa Palo*, Bharati Vidyapeeth College of Engineering, A-4, Paschim Vihar, New Delhi 110063, India, e-mail: nishi.deepa@nsut.ac.in; *Jasobanta Jena*, Institute of Mathematics and Application, Andharua, Bhubaneswar, Odisha 751029, India, e-mail: jjena67@gmail.com; *Meera Chadha* (corresponding author), DST Centre of Excellence in Climate Modeling, Indian Institute of Technology Delhi, Hauz Khas, New Delhi 110016, India, e-mail: meerachadha01@gmail.com.